Progressive Deformation of the Optic Nerve Head and Peripapillary Structures by Graded Horizontal Duction

Soh Youn Suh,[1] Alan Le,[1,2] Andrew Shin,[1] Joseph Park,[1,3] and Joseph L. Demer[1–6]

[1]Department of Ophthalmology, University of California, Los Angeles, California, United States
[2]Department of Neuroengineering, University of California, Los Angeles, California, United States
[3]Department of Bioengineering, University of California, Los Angeles, California, United States
[4]Stein Eye Institute, University of California, Los Angeles, California, United States
[5]Department of Neurology, University of California, Los Angeles, California, United States
[6]David Geffen Medical School, University of California, Los Angeles, California, United States

Correspondence: Joseph L. Demer, Stein Eye Institute, UCLA,100 Stein Plaza, Los Angeles, CA 90095-7002, USA;
jld@jsei.ucla.edu.

Submitted: July 11, 2017
Accepted: August 26, 2017

Citation: Suh SY, Le A, Shin A, Park J, Demer JL. Progressive deformation of the optic nerve head and peripapillary structures by graded horizontal duction. *Invest Ophthalmol Vis Sci*. 2017;58:5015–5021. DOI:10.1167/iovs.17-22596

Purpose. We investigated the effect of graded range of horizontal duction on the shape of the peripapillary Bruch's membrane (ppBM) and optic nerve head (ONH).

Methods. In 50 eyes of 25 normal subjects, the ONH and peripapillary retina were imaged by optical coherence tomography (OCT) in central gaze and incremental angles of add- and abduction. Displacements of the Bruch's membrane opening (BMO), optic cup (OC), and change in ONH angle in eccentric gazes were compared to those of central gaze, in add- and abduction.

Results. With increasing duction, the nasal edge of the BMO (nBMO) shifted progressively anteriorly in adduction and posteriorly in abduction, while the temporal edge of the BMO (tBMO) shifted posteriorly in adduction and anteriorly in abduction. The summed absolute nBMO and tBMO displacements in 30° and 35° adduction significantly exceeded those in comparable abduction angles ($P < 0.005$ for both). The ONH progressively tilted temporally in adduction and nasally in abduction; absolute ONH tilt in adduction was significantly greater than that in abduction for 30° and 35° ductions ($P < 0.005$ for both). BMO displacement and ONH tilt in adduction exhibited bilinear behavior, with greater effects for both at angles exceeding 26°. The OC shifted significantly farther anteriorly in abduction than adduction at every angle from 10° to 35°.

Conclusions. Horizontal duction deforms the ONH and ppBM, but more in adduction than in abduction, and increasingly so for angles greater than 26°. This behavior is consistent with optic nerve sheath tethering for adduction exceeding 26°.

Keywords: eye movements, optic nerve head, Bruch's membrane, optical coherence tomography

Magnetic resonance imaging (MRI) recently has demonstrated the novel finding that the optic nerve (ON) and its sheath become straightened and tether the globe during large angle ocular adduction.[1] While the ON and sheath are sinuous and redundant in central gaze and abduction, these structures straighten to minimum path length at a threshold adduction angle, after which further adduction requires a combination of ON elongation and globe displacement, including retraction. These effects imply that tractional force is exerted on the globe by the ON and sheath at angles exceeding the tethering threshold, estimated from MRI in normal subjects to be in the range of 22° to 26°. MRI provides evidence that this traction force induced by ON sheath tethering in adduction is focused mainly on the temporal optic nerve head (ONH) and peripapillary tissue, which correlates with the location of the peripapillary atrophy (PPA) observed typically in patients with glaucoma.[2–4] Therefore, this mechanical force exerted by the tethering ON has been suggested as a possible intraocular pressure (IOP)-independent mechanism of glaucomatous optic neuropathy.

This novel concept of ON tethering in adduction has been supported further by biomechanical studies using finite element analysis (FEA) of the mechanical stress (force/cross-sectional area) and strain (local deformation caused by stress) in the ONH during horizontal eye movement,[5,6] particularly in adduction.[7] While most prior biomechanical studies focused on the effects of IOP changes on the ONH,[8–12] these recent studies have suggested that deformation of the ONH caused by ON sheath traction in adduction is comparable or even greater than that induced by significant IOP elevation. However, biomechanical modeling by Wang et al.[6] of small horizontal ductions also has suggested that these eye movements may deform the ONH and peripapillary region even in the absence of ON tethering in adduction.[6]

Biomechanical effects of horizontal duction on the ONH and peripapillary tissue also have been demonstrated in vivo by optical coherence tomography (OCT) studies.[13–15] Sibony[13] used fixed angles of add- and abduction to demonstrate gaze-evoked deformation of the nasal and temporal peripapillary basement membranes in normal subjects that were greatly exaggerated in patients with papilledema. Wang et al.[14] demonstrated by OCT that fixed angles of moderate add- and abduction produce significant ONH strains in normal subjects.

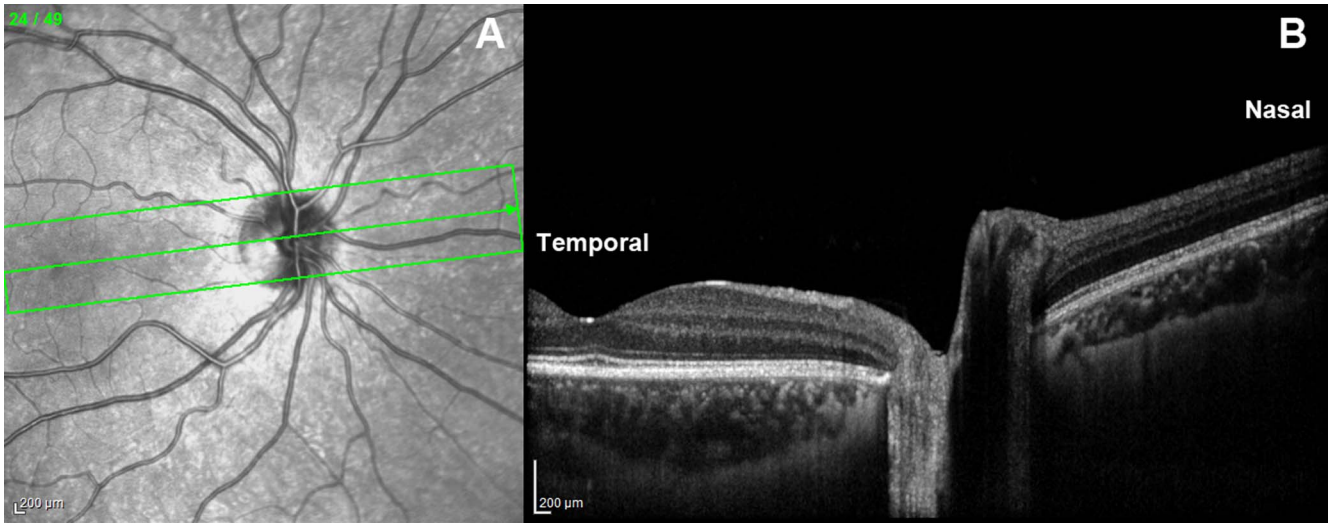

FIGURE 1. En face (A) and cross-sectional (B) OCT images of the ONH and peripapillary retina. The middle scan passing through the ONH center and foveola in (A) and shown in (B) was analyzed quantitatively. The aspect ratio in (B) is vertically exaggerated for illustrative purposes.

However, these OCT studies did not parameterize graded angles of ocular duction, and thus could not evaluate possible gradual or threshold effects of eye movement.

In our earlier OCT study, we reported progressive tilting of the ONH along with displacement of peripapillary retina during a range of add- and abduction graded in 10° increments nominally up to a maximum of 30°.[15] However, the nominal central position for this study was relative to the craniotopic straight-ahead position, and did not account for an offset of as much as 17° of the internal fixation target in the OCT scanner, which biased fixation toward the nasal direction. It currently is recognized that this internal target position offset caused overestimation of adduction angles and underestimation of abduction angles. This adduction bias of central target position may be the reason that the earlier OCT study failed to demonstrate significant ONH deformation during abduction, and did not demonstrate a threshold effect during adduction.

The foregoing evidence supports the supposition that there may be two different mechanisms of horizontal duction-related ONH deformation: (1) a small angle mechanism acting similarly in add- and abduction, and (2) a threshold mechanism acting only after ON and sheath tethering occur in large angle adduction. Using a wider range of horizontal ductions in finer increments centered on an unbiased, straight-ahead eye position, we investigated the graded effect of horizontal eye movement on ONH and peripapillary retina and determined the possible threshold point of the tethering force exerted by the ON in adduction.

METHODS

Subjects

A total of 25 volunteers (11 male and 14 female; mean age, 44.0 ± 18.9 [SD]; range, 18–71) were recruited by advertising for this study. Subjects provided written, informed consent before participation according to a protocol approved by the University of California, Los Angeles Institutional Review Board conforming to the tenets of the Declaration of Helsinki. All subjects underwent comprehensive ophthalmic histories and examinations to verify absence of ocular abnormalities other than refractive error or pseudophakia, normal corrected visual acuity, normal IOP (<21 mm Hg) without evidence of glaucomatous optic neuropathy, and normal binocular alignment. All 50 eyes were included in the analysis. Mean spherical equivalent refractive error was −1.1 ± 2.8 (SD; range, +4.6 to −7.5) diopters.

Optical Coherence Tomography

A spectral domain (SD)–OCT scanner (Spectralis; Heidelberg Engineering, Heidelberg, Germany) was used for imaging after pupillary dilation using phenylephrine-HCl 2.5% drops. A retinal nerve fiber layer (RNFL) circular scan was performed first to verify normal RNFL thickness in each eye. Then, wide-field volume scans of the ONH and peripapillary retina were performed in both eyes in central gaze, adduction (10°, 20°, 25°, 30°, 35°, and 40° [when anatomically possible given the subject's facial anatomy]) and abduction (10°, 20°, 25°, 30°, and 35°) sequentially. The enhanced depth imaging (EDI) consisted of 49 horizontal B-scans covering a 30° × 5° rectangular region of the ONH and peripapillary retina, vertically spaced at 30 µm. The raster was rotated to align the center of the ONH with the fovea before each scan (Fig. 1). To scan in eccentric gazes, the OCT imager was rotated incrementally in yaw to angles marked with a goniometric scale on its vertically-oriented pivot. Subject's heads were fixed in the central position using cushions and straps, and subjects were instructed not to move from this position as they fixated on the internal scanner target inside the OCT imager, which moved to each desired duction angle. The scanner was designed to offset its internal fixation target nasally to scan the ONH. The angle of this offset was determined in preliminary scans in which subjects fixated a target approximately 3 m distant with the nonimaged fellow eye. Since this viewing condition is not associated with convergence, it was possible to position the horizontal location of the distant target iteratively until the fovea was centered in the OCT scan. This demonstrated that the internal target was offset by 12° nasally. This offset then was applied to the goniometer scale attached to the scanner pivot, and used for all subjects. Adduction angle of 40° was obtainable in only a minority of subjects (25 eyes) who had suitable facial anatomy, because the nose collided with the lens of the OCT scanner in the others. Abduction was limited to 35° due to a mechanical limit in the scanner pivot.

Investigative Ophthalmology & Visual Science

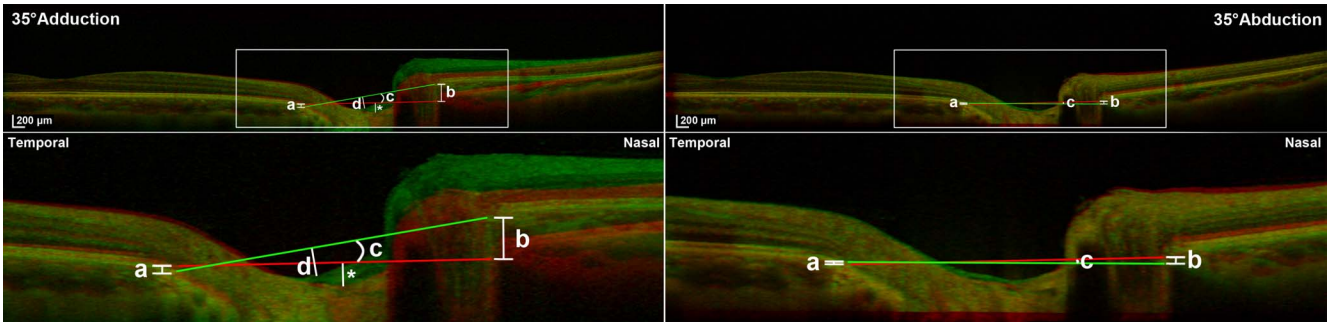

FIGURE 2. Superimposed OCT images of a right eye in central gaze (*red* reference image in all cases), 35° adduction (*green*, *left column*), and 35° abduction (*green*, *right column*). *Top row*: Ten mm-wide OCT scans. *Red* (central gaze) and *green lines* (eccentric gaze) connect nBMO and tBMO. *Bottom row*: Magnified views of rectangular area in *top* panels. *Left column*: In adduction, tBMO shifts posteriorly (a), nBMO shifts anteriorly (b), and ONH tilts temporally (c). Vertical distance from the BMO connecting line to the bottom of the OC was measured in central gaze (*) and in adduction (d) to determine the OC displacement. *Right column*: In abduction, tBMO shifts anteriorly (a), nBMO shifts posteriorly (b), and ONH tilts nasally (c). Note that the absolute BMO displacements and ONH tilt angles are greater in 35° adduction than in 35° abduction.

Image Analysis

From the 49 scans obtained for each eye in each gaze position, the scan including the center of the ONH and fovea was selected, exported as a TIFF file, and processed using Adobe Photoshop (Adobe Systems, San Jose, CA, USA). After correction of the aspect ratio that is vertically exaggerated in raw scanner images (Fig. 1B), images in central and eccentric gazes were colored differently in red or green for comparison in superimposable layers. Opacities of the images in eccentric gazes were reduced to 50% using the opacity function in Photoshop for superimposition by translation and rotation with the scans in central gaze, with the constraint that the far nasal and temporal peripheries of Bruch's membrane (BM; Fig. 2, top) be in complete alignment in the two gaze positions. While no absolute reference for ONH deformation was available as noted further in the Discussion, this approach provided a reference for displacement of the peripapillary region relative to relatively remote retinal locations presumed to be least likely to experience local deformation transmitted from the ONH. The remote nasal and temporal peripheral locations were used as reference points, since the direction of peripapillary retina displacement would otherwise depend on the choice of the reference.[15]

We analyzed three parameters for the scan in each eccentric gaze relative to central gaze: (1) displacement of the nasal and temporal edges of the BM opening (nBMO and tBMO), (2) change in ONH tilt angle as measured by the angle of a line connecting the nBMO and tBMO, and (3) displacement of the optic cup (OC) measured by the vertical distance from the deepest point of the OC to the line connecting the nBMO and tBMO. The BMO, the termination of BM at the ONH, was chosen for analysis because it is identified easily by SD-OCT and is an important anatomical structure through which the retinal nerve fibers pass.[16]

Statistical Analysis

Displacement from central gaze of the nBMO and tBMO, the change in ONH tilt angle, and the displacement of the OC were compared using paired *t*-tests. To account for interocular correlation between the two eyes of each subject, repeated analysis was performed using generalized estimating equations (GEE) with SPSS software (Version 24.0; IBM Corp., Armonk, NY, USA). For data sets that seemed monotonically bilinear, we summed coefficients of determination for linear fits to each data segment for all possible ranges of each fit, and considered the optimum transition point between fits to be that transition point resulting in the maximum summed coefficient of determination. The intersection of the two regression lines having the greatest summed coefficients of determination was considered to be the best estimate of the transition point between bilinear fits.

RESULTS

BMO Displacements

Deformation of the peripapillary region was consistently demonstrated by OCT in add- and abduction (Fig. 2). In adduction, nBMO shifted anteriorly and tBMO shifted posteriorly continuously with increasing angle (Fig. 3). Conversely, in abduction, nBMO shifted posteriorly and tBMO shifted anteriorly relative to central gaze (Fig. 3). Since nBMO and tBMO shifted in opposite directions, the sum of the absolute values of nBMO and tBMO displacement was compared between abduction and adduction. Total BMO displacement in adduction was significantly greater than in abduction for angles of 30° and 35° ($P = 0.004$ and $P = 0.003$, respectively, GEE). The summed nBMO and tBMO displacements were 75 ± 8 µm (mean ± SEM) and 107 ± 14 µm in 35° and 40° adduction, respectively, but only 51 ± 6 µm in 35° abduction.

The plots of BMO displacement in adduction illustrated in Figure 3 suggest bilinear behavior, with a low 1.2 rate of change in BMO displacement with gaze angle up to approximately 25°, and a higher 5.0 rate of change for larger angles where displacements in adduction significantly exceeded those in the same angles of abduction (Fig. 3). This suggestion was tested quantitatively by bilinear regression as described above. The intersection of the two best bilinear fits occurred at 25.7° adduction suggesting this angle as a threshold for behavioral transition.

ONH Tilt Angle

The ONH progressively tilted temporally in increasing adduction and reached 3.0° ± 0.4° in 40° adduction (Fig. 4). In abduction, ONH tilted nasally and the tilted angle measured 1.3° ± 0.1° in 35° abduction (Fig. 4). Similar to the pattern of BMO displacement, the absolute value of ONH tilt was significantly larger in 30° and 35° adduction than in comparable abduction ($P = 0.001$ and $P < 0.001$, respectively, GEE). Bilinear regression indicated that the slope of the relationship between ONH tilt and adduction was 0.03 below a transition point of 25.4° but 0.14 above this adduction angle, which is

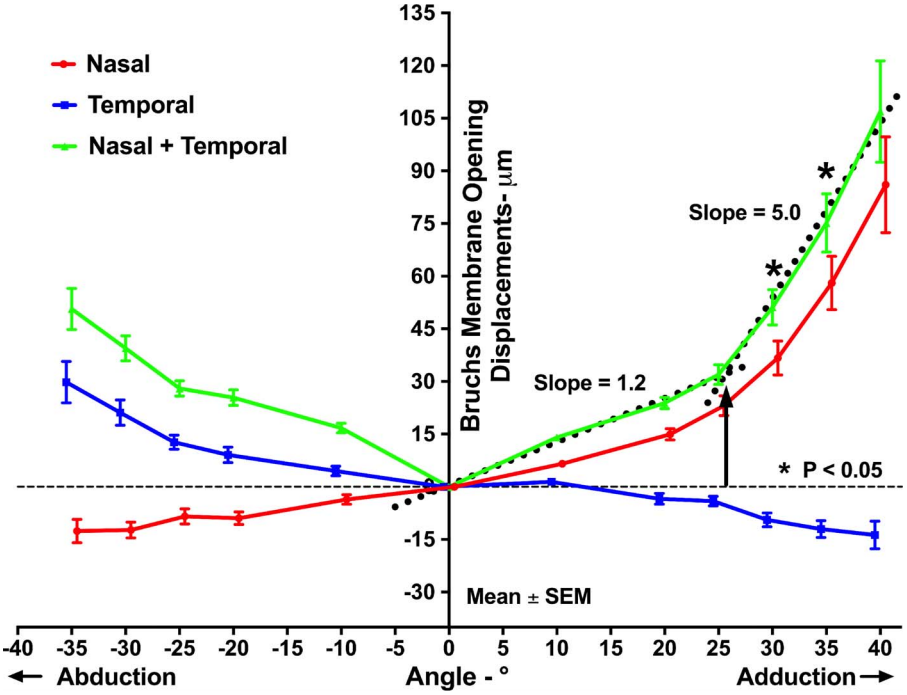

FIGURE 3. Mean displacements of nBMO and tBMO in add- and abduction. The summed absolute nBMO and tBMO displacements were significantly greater in adduction than in abduction at 30° and 35°. The intersection of the two best bilinear fits (*dotted lines*) to summed BMO displacements in adduction was at 25.7° (*black arrow*).

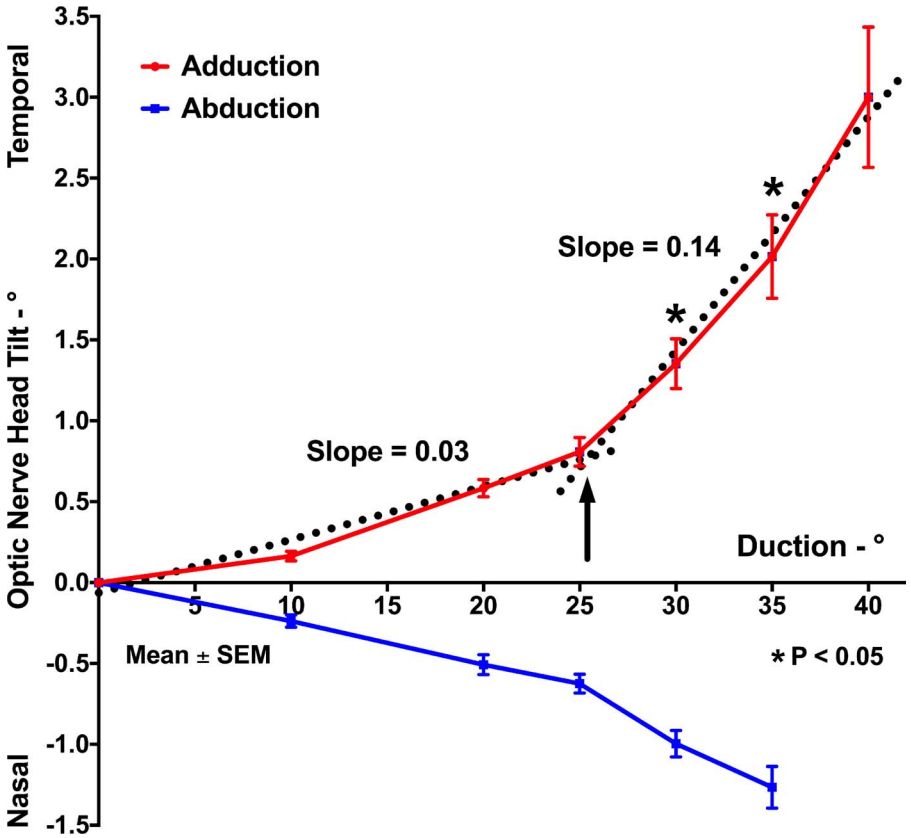

FIGURE 4. Mean ONH tilt in add- and abduction. The absolute tilt at 30° and 35° adduction was significantly greater than in comparable abduction. Bilinear regression of ONH tilt angle in adduction (*dotted lines*) indicated a transition point of 25.4° (*black arrow*).

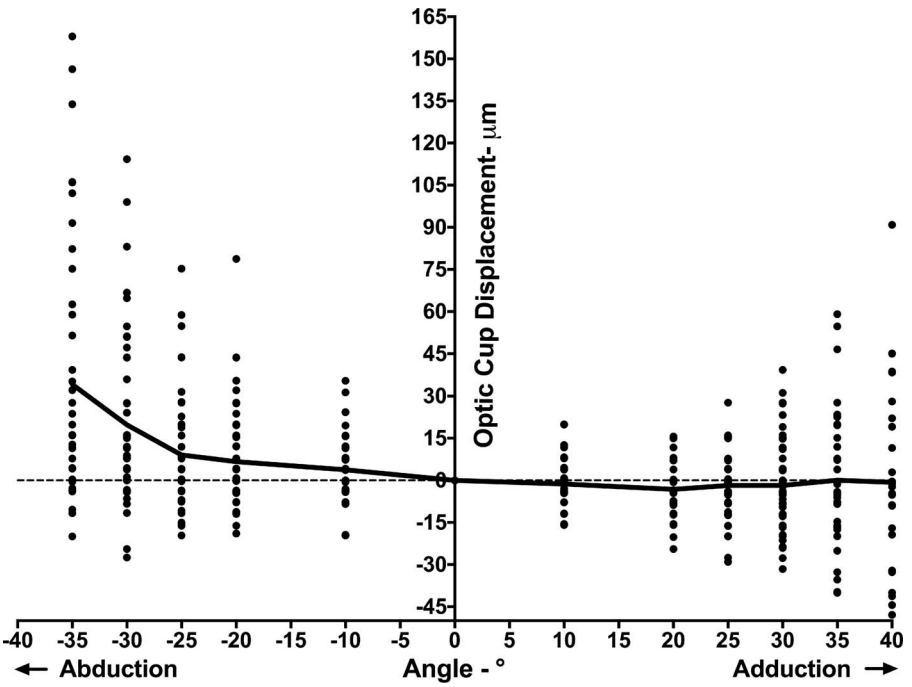

FIGURE 5. OC displacements in add- and abduction. Although displacements of OC varied widely among individuals, on average the OC shifted anteriorly in abduction, and showed little change in adduction.

similar to the transition adduction angle found for BMO displacement.

OC Displacement

The direction of OC displacement in eccentric gazes corresponded to the dominant direction of the peripapillary BM (ppBM) displacement. Thus, we considered that measuring the vertical distance from the line connecting nasal and temporal BMO points with the bottom of the OC would reflect the relative movement of the OC independently of shifts in the BMO. The OC position varied widely, particularly for large ductions, but there was a trend toward anterior OC displacement in abduction (Fig. 5). The difference in OC position between abduction and adduction was statistically significant at every angle from 10° to 35° ($P < 0.03$, GEE).

DISCUSSION

This study confirmed and extended the findings of earlier OCT studies[13–15] that horizontal eye rotation significantly deforms the ONH and peripapillary tissues. Adduction shifted the nBMO anteriorly, the tBMO posteriorly, and tilted the ONH temporally, while abduction caused converse behavior of each in the fashion described by Sibony as "seesaw."[13] While the displacement pattern of the OC during horizontal duction varied widely among subjects, the OC generally shifted farther anteriorly in abduction than adduction. This seesaw behavior was roughly linear with respect to gaze angle and was directionally symmetrical for add- and abduction. However, beyond approximately 26° adduction only, there was a significantly greater rate of BMO displacement and ONH tilt with further adduction, phenomena not evident for larger angles of abduction. This threshold for greater BMO displacement and ONH tilt beyond 26° adduction is consistent with adduction tethering by the ON and ON sheath demonstrated by MRI to occur at approximately this angle.[1]

The "seesaw-like" shape deformation of the BMO and ONH observed here might be explained by the stiffness of the ON sheath, as pressurized by cerebrospinal fluid (CSF) within it.[13] Elastin fibers embedded in the dense collagen matrix of the ON sheath have a mesh-like orientation consistent with high mechanical stiffness (Le A, et al. *IOVS*. 2017;58:ARVO E-Abstract 1736). The inner layer of the ON sheath that inserts on the scleral canal even has denser collagen and more elastin than the outer layer (Baig A, et al. *IOVS*. 2017;58:ARVO E-Abstract 1738). Given that ON sheath is much stiffer than the peripapillary sclera,[5–7] during horizontal duction the ON sheath would compress the peripapillary sclera on the side ipsilateral to the gaze direction, forcing the overlying ppBM anteriorly, while the ON sheath on the side contralateral to the gaze direction simultaneously exerts traction to drag the overlying ppBM posteriorly. These effects may be augmented by hydrostatic pressure of CSF stiffening the ON sheath. MRI demonstrates that CSF within the ON sheath shifts to the nasal side of the retrobulbar ON in adduction,[1] a shift that could compress the nasal peripapillary retina anteriorly. The foregoing is only one aspect of hydraulic stiffening of the ON sheath during horizontal duction, a concept further supported by Sibony's finding that the gaze-evoked seesaw deformations of the peripapillary region in papilledema are reduced after normalization of pathologically elevated intracranial pressure.[13] However, both of these effects should be similar in add- and abduction. For angles of 25° or more, neither ON sheath stiffness nor localized CSF pressure can explain the greater BM displacement and ONH tilting observed in adduction.

BM displacement and ONH tilt angle during graded range of adduction showed bilinear patterns suggesting existence of an alternative or supplemental mechanism of deformation beyond the 26° threshold, and this mechanism most likely is or includes ON and sheath tethering in adduction as demonstrated by MRI. Once the ON and its sheath lose redundancy and become straightened in adduction,[1] additional adduction causes the globe to retract, an effect especially prominent in

axial high myopia.[1] More recently, medial globe translation also has been demonstrated by MRI in adduction.[17] With the straightened ON sheath exerting traction on the temporal side of the ON and the globe simultaneously shifting posteronasally, the globe's rotational center shifts posterotemporally as the eye adducts, causing larger progressive displacements in the nasal than in the temporal peripapillary region. The sharply angulated anterior shifting of the nasal peripapillary retina in large adduction, termed "nasal buckling," occasionally observed in our earlier study[15] was indeed not a rare finding in the current study, but rather a general phenomenon. Our result suggested that the threshold of ON sheath tethering and possibly the globe translation occurs at approximately 26° in adduction, which matched to where the ON straightening was observed in normal controls by MRI.[1]

Significant temporal tilt of the ONH in adduction was confirmed again in the current study. Temporal ONH tilting along with temporal PPA is seen commonly in myopia,[18–22] which is a well-known risk factor of glaucoma.[23–25] Recent studies have shown that the presence of temporal ONH tilting and PPA are better associated with visual field defects and progression than the refractive error itself, implying that the structural change associated with myopia leads to glaucoma.[26,27] Although axial elongation of the globe has been suggested to cause ONH tilt and PPA,[22,28] there is no good explanation for why the tilting of the ONH and PPA predominantly occurs temporally in myopia and glaucoma. Our current finding suggested that ON sheath traction might be the primary cause of temporal ONH tilt considering that the pulling force induced by the tethered ON in adduction is exerted mainly on the temporal ONH and peripapillary region.[1] Furthermore, biomechanical modeling has predicted that ONH sheath tractional force in adduction is greatest at the temporal edge of the ON,[7] which also is the region where PPA generally occurs.

One might ask whether the reversible gaze-induced tiling of the ONH or the displacements of peripapillary BM presented in our study could lead to permanent anatomical deformations, and thus significantly damage these structures. As predicted by biomechanical modeling, ONH strain induced by horizontal duction can greatly exceed that induced by marked IOP elevation.[5,6] When this significant strain is repeated throughout the lifetime, repetitive strain injury might occur analogous to peripheral nerve injury observed with musculoskeletal disorders related to repetitive tasks.[29] As saccadic eye movements are reported to occur approximately 3 times per second,[30] it is plausible that adducting saccades accompanied by ONH tethering could cause remodeling of the ONH and peripapillary region and irreversibly damage these tissues.

A few limitations of the current study deserve consideration. In the earlier study, we commented that the directions of the peripapillary RPE and OC displacements necessarily depend on the chosen reference point if a single reference structure is used for analysis. In adduction, for example, the temporal RPE and OC shifted posteriorly when the nasal BM was used as a reference, but anteriorly when the temporal BM was used. The current study avoided the effect of arbitrary choice of reference by using the far nasal and temporal peripheral BM as dual reference points to investigate the directions of the ppBM and OC displacements in eccentric gazes. While a more robust approach, even these remote reference points still are within a 10-mm wide region of the posterior retina that also might have been subject to deformation by horizontal duction. Gaze-related deformation of even the remote nasal and temporal BM reference points would cause the current data to underestimate the reported effects in the peripapillary region. This limitation appears unavoidable at present, since a modern OCT scanner with widely-dilated pupil can maximally image only a 10-mm horizontal field region of the posterior eye. While MRI can image the whole orbit including the entire globe, the spatial resolution of even surface coil MRI in the range of 300 μm within 2 mm thick planes probably is insufficient for reliable measurement of ONH and peripapillary deformations that are in the range of tens of micrometers.

Although EDI-OCT was used in the current study, the high-speed mode slightly sacrificed resolution to minimize the scanning time as necessary to repetitively scan in numerous eccentric gazes. Deeper structures, such as lamina cribrosa (LC) or choroid, were not well visualized in every case, so those structures were not analyzed. Recently, posterior displacement of the LC and its reversal after IOP reduction have been demonstrated in OCT studies of glaucoma.[31–34] In future studies evaluating the possibility that ON tethering might constitute an IOP-independent mechanism of glaucomatous optic neuropathy, it would be useful to investigate whether horizontal eye movements deform the LC.

In conclusion, ocular rotation deforms the ONH and peripapillary region, significantly more so in adduction than in abduction. The displacement of ppBM and temporal tilting of the ONH that occurs symmetrically in both directions substantially increases beyond approximately 26° in adduction only, corresponding to the presumed threshold angle at which the ON sheath becomes selectively tethered in adduction. Further studies are needed to investigate whether these gaze-induced deformations of ONH and peripapillary tissue are abnormally great in glaucoma, which would test the novel hypothesis that ON sheath tethering occurring in adduction constitutes an IOP-independent mechanism of ON damage.

Acknowledgments

Supported by U.S. Public Health Service National Eye Institute Grant EY008313, and an unrestricted grant from Research to Prevent Blindness to the Department of Ophthalmology at the University of California, Los Angeles, CA, USA.

Disclosure: **S.Y. Suh**, None; **A. Le**, None; **A. Shin**, None; **J. Park**, None; **J.L. Demer**, None

References

1. Demer JL. Optic nerve sheath as a novel mechanical load on the globe in ocular duction. *Invest Ophthalmol Vis Sci*. 2016;57:1826–1838.
2. Park KH, Tomita G, Liou SY, Kitazawa Y. Correlation between peripapillary atrophy and optic nerve damage in normal-tension glaucoma. *Ophthalmology*. 1996;103:1899–1906.
3. Uchida H, Ugurlu S, Caprioli J. Increasing peripapillary atrophy is associated with progressive glaucoma. *Ophthalmology*. 1998;105:1541–1545.
4. Jonas JB. Clinical implications of peripapillary atrophy in glaucoma. *Curr Opin Ophthalmol*. 2005;16:84–88.
5. Wang X, Rumpel H, Lim WE, et al. Finite element analysis predicts large optic nerve head strains during horizontal eye movements. *Invest Ophthalmol Vis Sci*. 2016;57:2452–2462.
6. Wang X, Fisher LK, Milea D, Jonas JB, Girard MJ. Predictions of optic nerve traction forces and peripapillary tissue stresses following horizontal eye movements. *Invest Ophthalmol Vis Sci*. 2017;58:2044–2053.
7. Shin A, Yoo LH, Park J, Demer JL. Finite element biomechanics of optic nerve sheath traction in adduction. *J Biomech Eng*. 2017;139:101010.
8. Burgoyne CF, Downs JC, Bellezza AJ, Suh JK, Hart RT. The optic nerve head as a biomechanical structure: a new paradigm for understanding the role of IOP-related stress and

strain in the pathophysiology of glaucomatous optic nerve head damage. *Prog Retin Eye Res*. 2005;24:39–73.

9. Burgoyne CF, Downs JC. Premise and prediction-how optic nerve head biomechanics underlies the susceptibility and clinical behavior of the aged optic nerve head. *J Glaucoma*. 2008;17:318–328.
10. Sigal IA, Ethier CR. Biomechanics of the optic nerve head. *Exp Eye Res*. 2009;88:799–807.
11. Burgoyne CF. A biomechanical paradigm for axonal insult within the optic nerve head in aging and glaucoma. *Exp Eye Res*. 2011;93:120–132.
12. Nguyen TD, Ethier CR. Biomechanical assessment in models of glaucomatous optic neuropathy. *Exp Eye Res*. 2015;141:125–138.
13. Sibony PA. Gaze evoked deformations of the peripapillary retina in papilledema and ischemic optic neuropathy. *Invest Ophthalmol Vis Sci*. 2016;57:4979–4987.
14. Wang X, Beotra MR, Tun TA, et al. In vivo 3-dimensional strain mapping confirms large optic nerve head deformations following horizontal eye movements. *Invest Ophthalmol Vis Sci*. 2016;57:5825–5833.
15. Chang MY, Shin A, Park J, et al. Deformation of optic nerve head and peripapillary tissues by horizontal duction. *Am J Ophthalmol*. 2017;174:85–94.
16. Chauhan BC, Burgoyne CF. From clinical examination of the optic disc to clinical assessment of the optic nerve head: a paradigm change. *Am J Ophthalmol*. 2013;156:218–227.e2.
17. Demer JL, Clark RA, Suh SY, et al. Magnetic resonance imaging of optic nerve traction during adduction in primary open angle glaucoma with normal intraocular pressure. *Invest Ophthalmol Vis Sci*. 2017;58:4114–4125.
18. Vongphanit J, Mitchell P, Wang JJ. Population prevalence of tilted optic disks and the relationship of this sign to refractive error. *Am J Ophthalmol*. 2002;133:679–685.
19. Tay E, Seah SK, Chan SP, et al. Optic disk ovality as an index of tilt and its relationship to myopia and perimetry. *Am J Ophthalmol*. 2005;139:247–252.
20. Samarawickrama C, Mitchell P, Tong L, et al. Myopia-related optic disc and retinal changes in adolescent children from singapore. *Ophthalmology*. 2011;118:2050–2057.
21. You QS, Xu L, Jonas JB. Tilted optic discs: The Beijing Eye Study. *Eye*. 2008;22:728–729.
22. Kim TW, Kim M, Weinreb RN, Woo SJ, Park KH, Hwang JM. Optic disc change with incipient myopia of childhood. *Ophthalmology*. 2012;119:21–26.e3.
23. Marcus MW, de Vries MM, Junoy Montolio FG, Jansonius NM. Myopia as a risk factor for open-angle glaucoma: a systematic review and meta-analysis. *Ophthalmology*. 2011;118:1989–1994.e2.
24. Mitchell P, Hourihan F, Sandbach J, Wang JJ. The relationship between glaucoma and myopia: the Blue Mountains Eye Study. *Ophthalmology*. 1999;106:2010–2015.
25. Wong TY, Klein BE, Klein R, Knudtson M, Lee KE. Refractive errors, intraocular pressure, and glaucoma in a white population. *Ophthalmology*. 2003;110:211–217.
26. Sawada Y, Hangai M, Ishikawa M, Yoshitomi T. Association of myopic optic disc deformation with visual field defects in paired eyes with open-angle glaucoma: a cross-sectional study. *PLoS One*. 2016;11:e0161961.
27. Sawada Y, Hangai M, Ishikawa M, Yoshitomi T. Association of myopic deformation of optic disc with visual field progression in paired eyes with open-angle glaucoma. *PLoS One*. 2017;12:e0170733.
28. Jonas JB, Weber P, Nagaoka N, Ohno-Matsui K. Glaucoma in high myopia and parapapillary delta zone. *PLoS One*. 2017;12:e0175120.
29. Barr AE, Barbe MF. Pathophysiological tissue changes associated with repetitive movement: a review of the evidence. *Phys Ther*. 2002;82:173–187.
30. Wu CC, Kowler E. Timing of saccadic eye movements during visual search for multiple targets. *J Vis*. 2013;13(11):11.
31. Lee EJ, Kim TW, Weinreb RN. Reversal of lamina cribrosa displacement and thickness after trabeculectomy in glaucoma. *Ophthalmology*. 2012;119:1359–1366.
32. Lee EJ, Kim TW, Weinreb RN, Kim H. Reversal of lamina cribrosa displacement after intraocular pressure reduction in open-angle glaucoma. *Ophthalmology*. 2013;120:553–559.
33. Barrancos C, Rebolleda G, Oblanca N, Cabarga C, Munoz-Negrete FJ. Changes in lamina cribrosa and prelaminar tissue after deep sclerectomy. *Eye*. 2014;28:58–65.
34. Lee EJ, Kim TW. Lamina cribrosa reversal after trabeculectomy and the rate of progressive retinal nerve fiber layer thinning. *Ophthalmology*. 2015;122:2234–2242.

Investigative Ophthalmology & Visual Science